

# Out-of-domain Generalization from a Single Source: A Uncertainty Quantification Approach

Xi Peng, Fengchun Qiao and Long Zhao

**Abstract**—We study a worst-case scenario in generalization: Out-of-domain generalization from a single source. The goal is to learn a robust model from a single source and expect it to generalize over many unknown distributions. This challenging problem has been seldom investigated while existing solutions suffer from various limitations such as the ignorance of uncertainty assessment and label augmentation. In this paper, we propose uncertainty-guided domain generalization to tackle the aforementioned limitations. The key idea is to augment the source capacity in both feature and label spaces, while the augmentation is guided by uncertainty assessment. To the best of our knowledge, this is the first work to (1) quantify the generalization uncertainty from a single source and (2) leverage it to guide both feature and label augmentation for robust generalization. The model training and deployment are effectively organized in a Bayesian meta-learning framework. We conduct extensive comparisons and ablation study to validate our approach. The results prove our superior performance in a wide scope of tasks including image classification, semantic segmentation, text classification, and speech recognition.

**Index Terms**—Domain Generalization, Bayesian Inference, Adversarial Training, Meta-Learning, Uncertainty Quantification

arXiv:2108.02888v1 [cs.CV] 5 Aug 2021

## 1 INTRODUCTION

Existing machine learning algorithms have achieved remarkable success under the assumption that training and test data are sampled from similar distributions. When this assumption no longer holds, even strong models (e.g., deep neural networks) may fail to produce reliable predictions. In this paper, we study a worst-case scenario in generalization: *Out-of-domain inference from a single source*. A model learned from a single source is expected to generalize over a series of unknown distributions. This problem is more challenging than *Domain Adaptation* [40], [47], [50], [74] which usually requires the assessment of target distributions during training, and *Domain Generalization* [5], [10], [15], [38], [49] which often assumes the availability of multiple sources. The difference of the three problems is illustrated in Fig. 1.

Recently, GUD [71] casts this problem in an ensemble framework. It learns a group of models each of which tackles an unseen test domain. This is achieved by performing *Adversarial Training* [17] on the source to mimic the unseen test distributions. Yet, its generalization capability is limited due to the proposed semantic constraint, which allows only a small amount of data augmentation to avoid semantic changes in the label space. To address this limitation, M-ADA [52] proposes *Adversarial Domain Augmentation* to relax the constraint. By maximizing the Wasserstein distance between the source and augmentation, the domain transportation is significantly enlarged in the input space.

However, existing data (domain) augmentation based methods [7], [9], [24], [52], [71], [78] merely consider to increase the source capacity by perturbing the input space.

- Xi Peng is with the Department of Computer and Information Sciences, University of Delaware. DE, USA. E-mail: xipeng@udel.edu.
- Fengchun Qiao is with the Department of Computer and Information Sciences, University of Delaware. DE, USA. E-mail: fengchun@udel.edu.
- Long Zhao is with the Department of Computer Science, Rutgers University, NJ, USA. E-mail: lz311@cs.rutgers.edu.

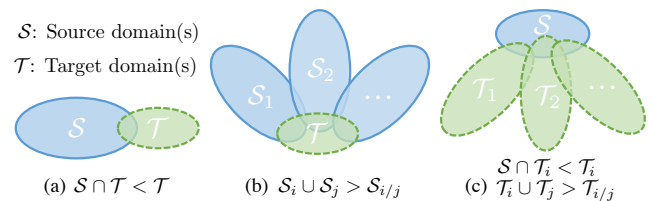


Fig. 1: The domain discrepancy: (a) domain adaptation, (b) domain generalization, and (c) single source generalization.

Few of them investigate the possibility of label space augmentation. An exception is *Mixup* [77] which pioneers label augmentation by randomly interpolating two data examples in both input and label spaces. However, Mixup can hardly address the out-of-domain inference problem since it is restricted in creating in-domain generations due to the linear interpolation assumption. Besides, the interpolations are randomly sampled from a fix distribution, which also largely restricts the flexibility of domain mixtures, yielding sub-optimal performance for unseen domain generalization.

Another limitation of existing work [5], [10], [15], [38], [49] is they usually overlook the potential risk of leveraging augmented data in tackling out-of-domain generalization. This raises serious safety and security concerns in mission-critical applications [12]. For instance, when deploying self-driving cars in unknown environments, it is crucial to be aware of the predictive uncertainty in risk assessment.

To tackle the aforementioned limitations, we propose uncertain out-of-domain generalization. The key idea is to increase the source capacity guided by uncertainty estimation in both feature and label spaces. More specifically, in the feature space, instead of directly augmenting raw data [52], [71], we apply uncertainty-guide perturbations to latent features, yielding a domain-knowledge-free solution for various modalities such as image, text, and audio. In the label space, we leverage the uncertainty associated with

feature perturbations to augment labels via interpolation, improving generalization over unseen domains. Moreover, we explicitly model the domain uncertainty as a byproduct of feature perturbation and label mixup, guaranteeing fast risk assessment without repeated sampling. Finally, we organize the training and deployment in a Bayesian meta-learning framework that is specially tailored for single source generalization.

This work features several extensions to our conference publication [52]. First, we propose a new method to efficiently quantify the generalization uncertainty from a single source and leverage it to guide model generalization. Second, we propose to jointly perturb both latent features and ground-truth labels to encourage substantial domain augmentations for out-of-domain generalization. Third, we redesign the implementation for a generic solution that can tackle a variety of data modalities including visual, audio, and textual data such as *Google Commands* [73] and *Amazon Reviews* [6]. Last but not least, we add comprehensive evaluations by comparing our method with baselines including comparing to adversarial training [23], [43], [72] and data augmentation [5], [7], [9], [77]. To summarize, our contribution is multi-fold:

- To the best of our knowledge, we are the first to quantify the generalization uncertainty from a single source. We leverage the uncertainty assessment to gradually improve the domain generalization in a curriculum learning scheme.
- For the first time, we propose learnable label mixup in addition to widely used input augmentation, further increasing the domain capacity and reinforcing generalization over unseen domains.
- We propose a Bayesian meta-learning method to effectively organize domain augmentation and model training. Bayesian inference is crucial in maximizing the posterior of domain augmentations, such that they can approximate the distribution of unseen domains.
- Extensive comparisons and ablation study prove our superior performance in a wide scope of tasks including image classification, semantic segmentation, text classification, and speech recognition.

## 2 RELATED WORK

In this section, we first review recent progress on domain adaptation and domain generalization, especially in the area of object recognition. Then, we briefly discuss previous works on adversarial training, meta-learning and uncertainty assessment, which are closely related to our method.

**Domain adaptation.** Domain discrepancy brought by domain or covariance shifts [64] severely degrades the model performance on cross-domain recognition. The models trained using Empirical Risk Minimization [30] usually perform poorly on unseen domains. To reduce the discrepancy across domains, a series of methods are proposed for unsupervised [13], [50], [55], [57], [60] or supervised domain adaptation [48], [74]. In unsupervised domain adaptation, works in this field mostly attempt to match the distribution of the target domain to that of the source domain by minimizing the maximal mean discrepancy [55] or a domain classifier network [40]. In supervised domain adaptation, some recent work focused on few-shot domain adaptation [47] where only

a few labeled samples from target domain are involved in training. The source and target domains are strongly coupled in both scenarios, limiting their generalization ability to other target domains. In this work, we expect the model to generalize well on many unseen target domains.

**Domain generalization.** Domain generalization [5], [10], [15], [20], [37], [59] is another line of research, which has been intensively studied in recent years. Different from domain adaptation, domain generalization aims to learn from multiple source domains without any access to target domains. Most previous methods either tried to learn a domain-invariant space to align domains [15], [20], [37], [49], [79] or aggregate domain-specific modules [44], [45]. A few studies [5], [52], [59], [71], [78] proposed data augmentation strategies to generate additional training data to enhance the generalization capability over unseen domains. JiGen [5] proposed to generate jigsaw puzzles from source domains and leverage them as self-supervised signals. CrossGrad [59] augments input instances with domain-guided perturbations through an auxiliary domain classifier. GUD [71] proposed adversarial data augmentation to solve single domain generalization, and learned an ensemble model for stable training. M-ADA [52] extended it to create augmentations with large domain transportation, and designed an efficient meta-learning scheme within a single unified model. Both GUD [71] and M-ADA [52] generate augmentations only in input space, while our method increases the augmentation capacity in both input and label space. Several methods [23], [43], [72] proposed to leverage adversarial training [17] to learn robust models, which can also be applied in single domain generalization. PAR [72] proposed to learn robust global representations by penalizing the predictive power of local representations. Hendrycks *et al.* [23] applied self-supervised learning to improve the model robustness.

**Adversarial training.** Adversarial training was originally proposed by [66]. They discovered that deep neural networks, including state-of-the-art models, are particularly vulnerable to minor adversarial perturbations. Goodfellow *et al.* [17] proposed Fast Gradient Sign Method (FGSM) which takes the sign of a gradient obtained from the classifier. FGSM made the model robust against adversarial samples and improved generalization performance. Madry *et al.* [43] illustrated that adversarial samples generated through projected gradient descent can provide robustness guarantees. Miyato *et al.* [46] proposed virtual adversarial training to smooth the output distributions as a regularization of models. Sinha *et al.* [61] proposed principled adversarial training with robustness guarantees through distributionally robust optimization. More recently, Stutz *et al.* [63] illustrated that on-manifold adversarial samples can improve generalization. Therefore, models with both robustness and generalization can be achieved at the same time. In our work, we leverage adversarial training to create feature perturbations for domain augmentation instead of directly perturbing raw data.

**Meta-learning.** Meta-learning [58], [67] is a long standing topic on learning models to generalize over a distribution of tasks. It has been widely used in optimization of deep neural networks [1], [39] and few-shot classification [29], [62], [70]. Recently, Finn *et al.* [11] proposed a Model-Agnostic Meta-Learning (MAML) procedure for few-shot learning and reinforcement learning. The objective of MAML is to

find a good initialization which can be fast adapted to new tasks within few gradient steps. In this paper, we propose a modified MAML to make the model generalize over the distribution of domain augmentation. Several approaches [2], [10], [38] have been proposed to learn domain generalization in a meta-learning framework. Li *et al.* [38] firstly applied MAML in domain generalization by adopting an episodic training paradigm. Balaji *et al.* [2] proposed to meta-learn a regularization function to train networks which can be easily generalized to different domains. Dou *et al.* [10] incorporated global and local constraints for learning semantic feature spaces in a meta-learning framework. However, these methods cannot be directly applied for single source generalization since there is only one distribution available during training.

**Uncertainty quantification.** Bayesian neural networks [4], [19], [25] have been intensively studied to integrate uncertainty into weights of deep networks. Instead, we apply Bayesian inference to quantify the uncertainty of domain augmentations. Several Bayesian meta-learning frameworks [12], [18], [35], [75] have been proposed to model the uncertainty of few-shot tasks. Grant *et al.* [18] proposed the first Bayesian variant of MAML [11] using the Laplace approximation. Yoon *et al.* [75] proposed a novel Bayesian MAML with a stein variational inference framework and chaser loss. Finn *et al.* [12] approximated MAP inference of the task-specific weights while maintain uncertainty only in the global weights. Lee *et al.* [35] proposed a Bayesian meta-learning framework to deal with class/task imbalance and out-of-distribution tasks. Lee *et al.* [36] proposed meta-dropout which generates learnable perturbations to regularize few-shot learning models. In this paper, instead of modelling the uncertainty of tasks, we propose a novel Bayesian meta-learning framework to maximize the posterior distribution of domain augmentations.

### 3 SINGLE DOMAIN GENERALIZATION

We aim at solving the problem of single domain generalization: A model is trained on only one source domain  $\mathcal{S}$  but is expected to generalize over a *unknown* domain distribution  $\{\mathcal{T}_1, \mathcal{T}_2, \dots\} \sim p(\mathcal{T})$ . This problem is more challenging than *domain adaptation* (assume  $p(\mathcal{T})$  is given) and *domain generalization* (assume multiple source domains  $\{\mathcal{S}_1, \mathcal{S}_2, \dots\}$  are available). A promising solution of this challenging problem, inspired by many recent achievements [40], [53], [71], is to leverage adversarial training [17], [66]. The key idea is to learn a robust model that is resistant to out-of-distribution perturbations. More specifically, we can learn the model by solving a worst-case problem [61]:

$$\min_{\theta} \sup_{\mathcal{T}: D(\mathcal{S}, \mathcal{T}) \leq \rho} \mathbb{E}[\mathcal{L}_{\text{task}}(\theta; \mathcal{T})], \quad (1)$$

where  $D$  is a similarity metric to measure the domain distance and  $\rho$  denotes the largest domain discrepancy between  $\mathcal{S}$  and  $\mathcal{T}$ .  $\theta$  are model parameters that are optimized according to a task-specific objective function  $\mathcal{L}_{\text{task}}$ . Here, we focus on classification problems using cross-entropy loss:

$$\mathcal{L}_{\text{task}}(\mathbf{y}, \hat{\mathbf{y}}) = - \sum_i y_i \log(\hat{y}_i), \quad (2)$$

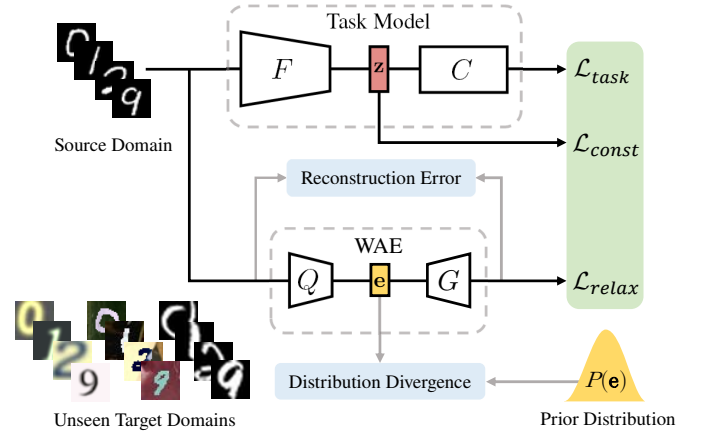


Fig. 2: Overview of adversarial domain augmentation. WAE is used to relax the semantic constraint and encourages large domain transportation.

where  $\hat{\mathbf{y}}$  is *softmax* output of the model;  $\mathbf{y}$  is the one-hot vector representing the ground truth class;  $y_i$  and  $\hat{y}_i$  represent the  $i$ -th dimension of  $\mathbf{y}$  and  $\hat{\mathbf{y}}$ , respectively.

Following the worst-case formulation (1), we propose a new method, *Meta-Learning based Adversarial Domain Augmentation* (M-ADA), for single domain generalization. Fig. 2 presents an overview of our approach. We create “fictitious” yet “challenging” domains by leverage adversarial training to augment the source domain in Sec. 3.1. The task model learns from the domain augmentations with the assistance of a Wasserstein Auto-Encoder (WAE), which relaxes the worst-case constraint in Sec. 3.2. We organize the joint training of task model and WAE, as well as the domain augmentation procedure, in a learning to learn framework as described in Sec. 3.3.

#### 3.1 Adversarial Domain Augmentation

Our goal is to create multiple augmented domains from the source domain. Augmented domains are required to be distributionally different from the source domain so as to mimic unseen domains. In addition, to avoid divergence of augmented domains, the worst-case guarantee defined in Eq. (1) should also be satisfied.

To achieve this goal, we propose Adversarial Domain Augmentation. Our model consists of a task model and a WAE shown in Fig. 2. In Fig. 2, the task model consists of a feature extractor  $F: \mathcal{X} \rightarrow \mathcal{Z}$  mapping images from input space to embedding space, and a classifier  $C: \mathcal{Z} \rightarrow \mathcal{Y}$  used to predict labels from embedding space. Let  $\mathbf{z}$  denote the latent representation of  $\mathbf{x}$  which is obtained by  $\mathbf{z} = F(\mathbf{x})$ . The overall loss function is formulated as follows:

$$\mathcal{L}_{\text{ADA}} = \underbrace{\mathcal{L}_{\text{task}}(\theta; \mathbf{x})}_{\text{Classification}} - \alpha \underbrace{\mathcal{L}_{\text{const}}(\theta; \mathbf{z})}_{\text{Constraint}} + \beta \underbrace{\mathcal{L}_{\text{relax}}(\psi; \mathbf{x})}_{\text{Relaxation}}, \quad (3)$$

where  $\mathcal{L}_{\text{task}}$  is the classification loss defined in Eq. (2),  $\mathcal{L}_{\text{const}}$  is the worst-case guarantee defined in Eq. (1), and  $\mathcal{L}_{\text{relax}}$  guarantees large domain transportation defined in Eq. (7).  $\psi$  are parameters of the WAE.  $\alpha$  and  $\beta$  are two hyper-parameter to balance  $\mathcal{L}_{\text{const}}$  and  $\mathcal{L}_{\text{relax}}$ .

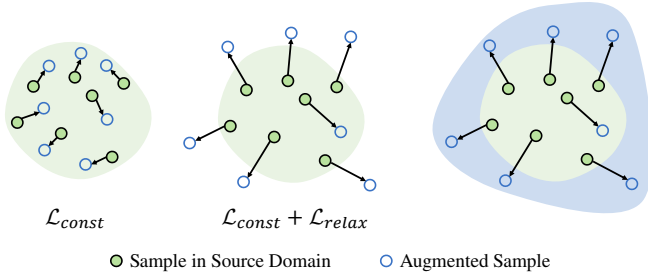


Fig. 3: Motivation of  $\mathcal{L}_{\text{relax}}$ . **Left:** The augmented samples may be close to the source domain if applying  $\mathcal{L}_{\text{const}}$ . **Middle:** We expect to create out-of-domain augmentations by incorporating  $\mathcal{L}_{\text{relax}}$ . **Right:** This would yield an enlarged training domain.

Given the objective function  $\mathcal{L}_{\text{ADA}}$ , we employ an iterative way to generate the adversarial samples  $\mathbf{x}^+$  in the augmented domain  $\mathcal{S}^+$ :

$$\mathbf{x}_{t+1}^+ \leftarrow \mathbf{x}_t^+ + \gamma \nabla_{\mathbf{x}_t^+} \mathcal{L}_{\text{ADA}}(\theta, \psi; \mathbf{x}_t^+, \mathbf{z}_t^+), \quad (4)$$

where  $\gamma$  is the learning rate of gradient ascent. A small number of iterations are required to produce sufficient perturbations and create desirable adversarial samples.

$\mathcal{L}_{\text{const}}$  imposes semantic consistency constraint to adversarial samples so that  $\mathcal{S}^+$  satisfies  $D(\mathcal{S}, \mathcal{S}^+) \leq \rho$ . More specifically, we follow [71] to measure the Wasserstein distance between  $\mathcal{S}^+$  and  $\mathcal{S}$  in the embedding space:

$$\mathcal{L}_{\text{const}} = \frac{1}{2} \|\mathbf{z} - \mathbf{z}^+\|_2^2 + \infty \cdot \mathbf{1}\{\mathbf{y} \neq \mathbf{y}^+\}, \quad (5)$$

where  $\mathbf{1}\{\cdot\}$  is the 0-1 indicator function and  $\mathcal{L}_{\text{const}}$  will be  $\infty$  if the class label of  $\mathbf{x}^+$  is different from  $\mathbf{x}$ . We assume  $\mathbf{y}^+ = \mathbf{y}$  is always true given a small enough step size, which simplifies implementation without compromising performance. Intuitively,  $\mathcal{L}_{\text{const}}$  controls the ability of generalization outside the source domain measured by Wasserstein distance [69]. In the conventional setting of adversarial training, the worst-case problem is handled by only  $\mathcal{L}_{\text{task}}$  and  $\mathcal{L}_{\text{const}}$ . However,  $\mathcal{L}_{\text{const}}$  yields limited domain transportation since it severely constrains the semantic distance between the samples and their perturbations. Hence,  $\mathcal{L}_{\text{relax}}$  is proposed to relax the semantic consistency constraint and create large domain transportation. The implementation of  $\mathcal{L}_{\text{relax}}$  is discussed in Sec. 3.2.

### 3.2 Relaxation of Wasserstein Distance Constraint

Intuitively, we expect the augmented domains  $\mathcal{S}^+$  are largely different from the source domain  $\mathcal{S}$ . In other words, we want to maximize the domain discrepancy between  $\mathcal{S}^+$  and  $\mathcal{S}$ . However, the semantic consistency constraint  $\mathcal{L}_{\text{const}}$  would severely limit the domain transportation from  $\mathcal{S}$  to  $\mathcal{S}^+$ , posing new challenges to generate desirable  $\mathcal{S}^+$ . To address this issue, we propose  $\mathcal{L}_{\text{relax}}$  to encourage out-of-domain augmentations. We illustrate the idea in Fig. 3.

Specifically, we employ Wasserstein Auto-Encoders (WAEs) [68] to implement  $\mathcal{L}_{\text{relax}}$ . Let  $V$  denote the WAE parameterized by  $\psi$ .  $V$  consists of an encoder  $Q(\mathbf{e}|\mathbf{x})$  and a decoder  $G(\mathbf{x}|\mathbf{e})$  where  $\mathbf{x}$  and  $\mathbf{e}$  denote inputs and bottleneck embedding, respectively. Additionally, we use a distance

---

**Algorithm 1:** The proposed Meta-Learning based Adversarial Domain Augmentation (M-ADA).

---

**Input:** Source domain  $\mathcal{S}$ ; Pre-train WAE  $V$  on  $\mathcal{S}$ ;  
Number of augmented domains  $K$

**Output:** Learned model parameters  $\theta$

```

1 for  $k = 1, \dots, K$  do
2   Generate  $\mathcal{S}_k^+$  from  $\mathcal{S} \cup \{\mathcal{S}_i^+\}_{i=1}^{k-1}$  using Eq. (4)
3   Re-train  $V$  with  $\mathcal{S}_k^+$ 
4   Meta-train: Evaluate  $\mathcal{L}_{\text{task}}(\theta; \mathcal{S})$  w.r.t  $\mathcal{S}$ 
5   Compute  $\hat{\theta}$  using Eq. (8)
6   for  $i = 1, \dots, k$  do
7     Meta-test: Evaluate  $\mathcal{L}_{\text{task}}(\hat{\theta}; \mathcal{S}_i^+)$  w.r.t  $\mathcal{S}_i^+$ 
8   end
9   Meta-update: Update  $\theta$  using Eq. (9)
10 end

```

---

metric  $\mathcal{D}_e$  to measure the divergence between  $Q(\mathbf{x})$  and a prior distribution  $P(\mathbf{e})$ , which can be implemented as either *Maximum Mean Discrepancy* (MMD) or GANs [16]. We can learn  $V$  by optimizing:

$$\min_{\psi} [\|G(Q(\mathbf{x})) - \mathbf{x}\|^2 + \lambda \mathcal{D}_e(Q(\mathbf{x}), P(\mathbf{e}))], \quad (6)$$

where  $\lambda$  is a hyper-parameter. After pre-training  $V$  on the source domain  $\mathcal{S}$  offline, we keep it frozen and maximize the reconstruction error  $\mathcal{L}_{\text{relax}}$  for domain augmentation:

$$\mathcal{L}_{\text{relax}} = \|\mathbf{x}^+ - V(\mathbf{x}^+)\|^2. \quad (7)$$

Different from Vanilla or Variation Auto-Encoders [28], WAEs employ the Wasserstein metric to measure the distribution distance between the input and reconstruction. Hence, the pre-trained  $V$  can better capture the distribution of the source domain and maximizing  $\mathcal{L}_{\text{relax}}$  creates large domain transportation.

In this work,  $V$  acts as a *one-class discriminator* to distinguish whether the augmentation is outside the source domain, which is significantly different from the traditional discriminator of GANs [16]. And it is also different from the domain classifier widely used in domain adaptation [40], since there is only one source domain available. As a result,  $\mathcal{L}_{\text{relax}}$  together with  $\mathcal{L}_{\text{const}}$  are used to “push away”  $\mathcal{S}^+$  in input space and “pull back”  $\mathcal{S}^+$  in the embedding space simultaneously.

### 3.3 Meta-Learning Single Domain Generalization

To efficiently organize the model training on the source domain  $\mathcal{S}$  and augmented domains  $\mathcal{S}^+$ , we leverage a meta-learning scheme to train a single model. To mimic real domain-shifts between the source domain  $\mathcal{S}$  and target domain  $\mathcal{T}$ , at each learning iteration, we perform meta-train on the source domain  $\mathcal{S}$  and meta-test on all augmented domains  $\mathcal{S}^+$ . Hence, after many iterations, the model is expected to achieve good generalization on the final target domain  $\mathcal{T}$  during evaluation.

Formally, the proposed Meta-Learning based Adversarial Domain Augmentation (M-ADA) approach consists of three parts in each iteration during the training procedure: meta-train, meta-test and meta-update. In meta-train,  $\mathcal{L}_{\text{task}}$  is

computed on samples from the source domain  $\mathcal{S}$ , and the model parameters  $\theta$  is updated via one or more gradient steps with a learning rate of  $\eta$ :

$$\hat{\theta} \leftarrow \theta - \eta \nabla_{\theta} \mathcal{L}_{\text{task}}(\theta; \mathcal{S}). \quad (8)$$

Then we compute  $\mathcal{L}_{\text{task}}(\hat{\theta}; \mathcal{S}_k^+)$  on each augmented domain  $\mathcal{S}_k^+$  in meta-test. At last, in meta-update, we update  $\theta$  by the gradients calculated from a combined loss where meta-train and meta-test are optimised simultaneously:

$$\theta \leftarrow \theta - \eta \nabla_{\theta} [\mathcal{L}_{\text{task}}(\theta; \mathcal{S}) + \sum_{k=1}^K \mathcal{L}_{\text{task}}(\hat{\theta}; \mathcal{S}_k^+)], \quad (9)$$

where  $K$  is the number of augmented domains. Note that in addition to the augmented domains  $\mathcal{S}^+$ , we also minimize the loss on the source domain  $\mathcal{S}$  to avoid performance degradation when  $\mathcal{S}^+$  are far away from  $\mathcal{S}$ .

The entire training pipeline is summarized in Alg. 1. In contrast to prior work [71] that learns a series of ensemble models, our method achieves a single model for efficiency. More importantly, the meta-learning scheme prepares the learned model for fast adaptation: One or a small number of gradient steps will produce improved behavior on a new target domain. This enables M-ADA for *few-shot domain adaptation*. Please refer to Sec 6.1 for more details.

## 4 UNCERTAIN OUT-OF-DOMAIN GENERALIZATION

M-ADA has achieved great success in single domain generalization. We propose to further improve M-ADA for out-of-domain generalization tasks.

**Uncertainty-guided domain generalization.** We assume that  $\mathcal{S}^+$  should integrate uncertainty assessment for efficient domain generalization. To achieve it, we introduce the auxiliary  $\psi = \{\phi_p, \phi_m\}$  to explicitly model the uncertainty with respect to  $\theta$  and leverage it to create  $\mathcal{S}^+$  by increasing the capacity in both input and label spaces. In input space, we introduce  $\phi_p$  to create feature augmentations  $\mathbf{h}^+$  via adding perturbation  $\mathbf{e}$  sampled from  $\mathcal{N}(\boldsymbol{\mu}, \boldsymbol{\sigma})$ . In label space, we integrate the same uncertainty encoded in  $(\boldsymbol{\mu}, \boldsymbol{\sigma})$  into  $\phi_m$  and propose learnable mixup to generate  $\mathbf{y}^+$  (together with  $\mathbf{h}^+$ ) through three variables  $(a, b, \tau)$ , yielding consistent augmentation in both input and output spaces. To effectively organize domain augmentation and model training, we propose a Bayesian meta-learning framework to *maximizing a posterior* of  $p(\mathcal{S}^+)$  by jointly optimizing the backbone  $\theta$  and the auxiliary  $\psi$ . The overall framework is shown in Fig. 4.

**Merits of uncertainty quantification.** Uncertainty quantification plays a key role in our design. First, it provides consistent guidance to the augmentation in both input and label spaces when inferring  $\mathcal{S}^+$ , which has never been studied before. Second, we can gradually enlarge the domain transportation by increasing the uncertainty of  $\mathcal{S}^+$  in a curriculum learning scheme [3]. Last, we can easily assess the domain uncertainty by checking the value of  $\boldsymbol{\sigma}$ , which measures how unsure it is when deploying on unseen domains  $\mathcal{T}$  (Sec. 4.3).

### 4.1 Uncertainty-Guided Input Augmentation

The goal is to create  $\mathcal{S}^+$  from  $\mathcal{S}$  such that  $p(\mathcal{S}^+)$  can approximate the out-of-domain distribution of  $\mathcal{S}$ . One the

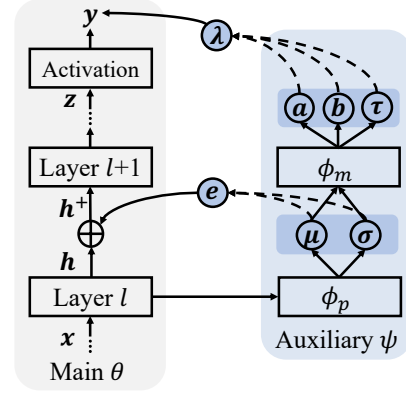


Fig. 4: The main and auxiliary models. The auxiliary model  $\phi$  is used to create uncertainty-guide augmentations in both feature and label spaces.

one hand, we expect a large domain transportation from  $\mathcal{S}$  to  $\mathcal{S}^+$  to best accommodate the unseen testing distribution  $p(\mathcal{T})$ . On the other hand, we prefer the transportation is domain-knowledge-free with uncertainty guarantee for broad and safe domain generalization. Towards this goal, we introduce  $\phi_p$  to create feature augmentation  $\mathbf{h}^+$  with large domain transportation through increasing the uncertainty with respect to  $\theta$ .

**Adversarial domain augmentation.** To encourage large domain transportation, we cast the problem in a worst-case scenario [61] and propose to learn the auxiliary mapping  $\phi_p$  via *adversarial domain augmentation*:

$$\underset{\phi_p}{\text{maximize}} \underbrace{\mathcal{L}(\theta; \mathcal{S}^+)}_{\text{Main task}} - \beta \underbrace{\|\mathbf{z} - \mathbf{z}^+\|_2^2}_{\text{Constraint}}. \quad (10)$$

Here,  $\mathcal{L}$  denotes empirical loss such as cross-entropy loss for classification. The second term is the worst-case constraint, bounding the largest domain discrepancy between  $\mathcal{S}$  and  $\mathcal{S}^+$  in embedding space.  $\mathbf{z}$  denotes the FC-layer output right before the activation layer, which is distinguished from  $\mathbf{h}$  that denotes the Conv-layer outputs.

One merit of the proposed uncertainty-guided augmentation is that we can effectively relax the constraint to encourage large domain transportation in a curriculum learning scheme, which is significantly more efficient than M-ADA [52] that has to train an extra WAE [68] to achieve this goal. We introduce the detailed form of  $\mathbf{h}^+$  as follows.

**Variational feature perturbation.** To achieve adversarial domain augmentation, we apply uncertainty-guided perturbations to latent features instead of directly augmenting raw data, yielding domain-knowledge-free augmentation. We propose to learn layer-wise feature perturbations  $\mathbf{e}$  that transport latent features  $\mathbf{h} \rightarrow \mathbf{h}^+$  for efficient domain augmentation  $\mathcal{S} \rightarrow \mathcal{S}^+$ . Instead of a direct generation  $\mathbf{e} = f_{\phi_p}(\mathbf{x}, \mathbf{h})$  widely used in previous work [52], [71], we assume  $\mathbf{e}$  follows a multivariate Gaussian distribution  $\mathcal{N}(\boldsymbol{\mu}, \boldsymbol{\sigma})$ , which can be used to easily access the uncertainty. More specifically, the Gaussian parameters are learnable via variational inference  $(\boldsymbol{\mu}, \boldsymbol{\sigma}) = f_{\phi_p}(\mathcal{S}, \theta)$ , such that:

$$\mathbf{h}^+ \leftarrow \mathbf{h} + \text{Softplus}(\mathbf{e}), \text{ where } \mathbf{e} \sim \mathcal{N}(\boldsymbol{\mu}, \boldsymbol{\sigma}), \quad (11)$$

where  $\text{Softplus}(\cdot)$  is applied to stabilize the training. Learning the variational distribution instead of a direct prediction of  $\mathbf{e}$  plays a key role in our design. First, it aims to model the overall distribution of perturbations of entire  $\mathcal{S}$  instead of an instance  $\mathbf{x}$ . Diverse perturbations can be sampled from the learned Gaussian distribution, allowing to explore more directions for augmentation. Second, we can easily assess the domain uncertainty by checking the values of  $\sigma$ , which measures how unsure it is when inferring a new domain  $\mathcal{S}^+$  (Sec. 4.3). Last but not least, we can efficiently sample many  $\mathcal{S}^+$  from a single  $\mathcal{S}$  to support the meta-learning scheme. Specifically, in each meta-learning iteration, we perform one-step meta-train on  $\mathcal{S}$  and many-steps meta-test on different  $\mathcal{S}^+$ , yielding more accurate gradient calculation over the aggregation of testing domains.  $\phi_p$  can create a series of feature augmentations  $\{\mathbf{h}_1^+, \mathbf{h}_2^+, \dots\}$  in different training iterations. In Sec. 6.5, we empirically show that  $\{\mathbf{h}_1^+, \mathbf{h}_2^+, \dots\}$  gradually enlarge the transportation through increasing the uncertainty of augmentations in a curriculum learning scheme and enable the model to learn from “easy” to “hard” domains.

## 4.2 Uncertainty-Guided Label Mixup

Feature perturbations do not only augment the input but also yield label uncertainty. To explicitly model the label uncertainty, we leverage the input uncertainty, encoded in  $(\boldsymbol{\mu}, \boldsymbol{\sigma})$ , to infer the label uncertainty encoded in  $(a, b, \tau)$  through  $\phi_m$  as shown in Fig. 4. We leverage the label uncertainty to propose learnable label mixup, yielding consistent augmentation in both input and output spaces and further reinforcing generalization over unseen domains.

**Random mixup.** We start by introducing random mixup [77] for robust learning. The key idea is to regularize the training to favor simple linear behavior in-between examples. More specifically, *mixup* performs training on convex interpolations of pairs of examples  $(\mathbf{x}_i, \mathbf{x}_j)$  and their labels  $(\mathbf{y}_i, \mathbf{y}_j)$ :

$$\mathbf{x}^+ = \lambda \mathbf{x}_i + (1 - \lambda) \mathbf{x}_j, \quad \mathbf{y}^+ = \lambda \mathbf{y}_i + (1 - \lambda) \mathbf{y}_j,$$

where  $\lambda \sim \text{Beta}(\alpha, \alpha)$  and the *mixup* hyper-parameter  $\alpha \in (0, +\infty)$  controls the interpolation strength.

**Learnable label mixup.** We improve *mixup* by casting it in a learnable framework specially tailored for single source generalization. First, instead of mixing up pairs of examples, we mix up  $\mathcal{S}$  and  $\mathcal{S}^+$  to achieve in-between domain interpolations. Second, we leverage the uncertainty encoded in  $(\boldsymbol{\mu}, \boldsymbol{\sigma})$  to predict learnable parameters  $(a, b)$ , which controls the direction and strength of domain interpolations:

$$\mathbf{h}^+ = \lambda \mathbf{h} + (1 - \lambda) \mathbf{h}^+, \quad \mathbf{y}^+ = \lambda \mathbf{y} + (1 - \lambda) \tilde{\mathbf{y}}, \quad (12)$$

where  $\lambda \sim \text{Beta}(a, b)$  and  $\tilde{\mathbf{y}}$  denotes a *label-smoothing* [65] version of  $\mathbf{y}$ . More specifically, we perform *label smoothing* by a chance of  $\tau$ , such that we assign  $\rho \in (0, 1)$  to the true category and equally distribute  $\frac{1-\rho}{c-1}$  to the others, where  $c$  counts categories. The Beta distribution  $(a, b)$  and the lottery  $\tau$  are jointly inferred by  $(a, b, \tau) = f_{\phi_m}(\boldsymbol{\mu}, \boldsymbol{\sigma})$  to integrate the uncertainty of domain augmentation. In Sec. 6.5, we empirically prove that the uncertainty encoded in  $\boldsymbol{\mu}$  and  $\boldsymbol{\sigma}$  can encourage more smoothing labels and significantly increase the capacity of label space.

## 4.3 A Unified Framework

To effectively organize domain augmentation and model training, we propose a Bayesian meta-learning framework to *maximize a posterior* of  $p(\mathcal{S}^+)$  by jointly optimizing the backbone  $\theta$  and the auxiliary  $\psi = \{\phi_p, \phi_m\}$ . Specifically, we *meta-train* the backbone  $\theta$  on the source  $\mathcal{S}$  and *meta-test* its generalization capability over  $p(\mathcal{S}^+)$ , where  $\mathcal{S}^+$  is generated by performing data augmentation in both input (Sec. 4.1) and output (Sec. 4.2) spaces through the auxiliary  $\psi$ . Finally, we *meta-update*  $\{\theta, \psi\}$  using gradient:

$$\nabla_{\theta, \psi} \mathbb{E}_{p(\mathcal{S}^+)} [\mathcal{L}(\theta^*; \mathcal{S}^+)], \text{ where } \theta^* \equiv \theta - \alpha \nabla_{\theta} \mathcal{L}(\theta; \mathcal{S}). \quad (13)$$

Here  $\theta^*$  is the meta-trained backbone on  $\mathcal{S}$  and  $\alpha$  is the learning rate. After training, the backbone  $\theta$  is expected to bound the generalization uncertainty over unseen populations  $p(\mathcal{T})$  in a worst-case scenario (Sec. 4.1) while  $\psi$  can be used to access the value of uncertainty efficiently.

**Bayesian meta-learning.** The goal is to maximize the conditional likelihood of the augmented domain  $\mathcal{S}^+$ :  $\log p(\mathbf{y}^+ | \mathbf{x}, \mathbf{h}^+; \theta^*)$ . However, solving it involves the true posterior  $p(\mathbf{h}^+ | \mathbf{x}; \theta^*, \psi)$ , which is intractable [35]. Thus, we resort to amortized variational inference with a tractable form of approximate posterior  $q(\mathbf{h}^+ | \mathbf{x}; \theta^*, \psi)$ . The approximated lower bound is as follows:

$$L_{\theta, \psi} = \mathbb{E}_{q(\mathbf{h}^+ | \mathbf{x}; \theta^*, \psi)} \left[ \log \frac{p(\mathbf{y}^+ | \mathbf{x}, \mathbf{h}^+; \theta^*)}{q(\mathbf{h}^+ | \mathbf{x}; \theta^*, \psi)} \right]. \quad (14)$$

We leverage Monte-Carlo (MC) sampling to maximize the lower bound  $L_{\theta, \psi}$  by:

$$\min_{\theta, \psi} \frac{1}{K} \sum_{k=1}^K [-\log p(\mathbf{y}_k^+ | \mathbf{x}, \mathbf{h}_k^+; \theta^*)] + \text{KL} [q(\mathbf{h}^+ | \mathbf{x}; \theta^*, \psi) \| p(\mathbf{h}^+ | \mathbf{x}; \theta^*, \psi)], \quad (15)$$

where  $\mathbf{h}_k^+ \sim q(\mathbf{h}^+ | \mathbf{x}; \theta^*, \psi)$  and  $K$  is the number of MC samples. For KL divergence, traditional Gaussian prior  $\mathcal{N}(\mathbf{0}, \mathbf{I})$  [28] is not compatible with our setup, since it may constrain the uncertainty of domain augmentations. Instead, we let  $q(\mathbf{h}^+ | \mathbf{x}; \theta^*, \psi)$  approximate  $p(\mathbf{h}^+ | \mathbf{x}; \theta^*, \psi)$  through adversarial training on  $\phi_p$  in Eq. 10, so that the learned adversarial distribution is more flexible to approximate unseen domains. Thanks to the Bayesian meta-learning framework, the generalization uncertainty on unseen domains is significantly suppressed (Sec. 6.5). More importantly, a few examples of the target domain can quickly adapt  $\theta$  to be domain-specific, yielding largely improved performance for few-shot domain adaptation (Sec. 6.1).

**Uncertainty estimation.** At testing time, given a novel domain  $\mathcal{T}$ , we propose a *normalized domain uncertainty score*,  $|\frac{\sigma(\mathcal{T}) - \sigma(\mathcal{S})}{\sigma(\mathcal{S})}|$ , to estimate its uncertainty with respect to learned  $\theta$ . Considering  $\psi$  is usually much smaller than  $\theta$ , this score can be calculated efficiently by one-pass data forwarding through  $\psi$ . In Sec. 6.1, we empirically prove that our estimation is consistent with conventional Bayesian methods [4], while the time consumption is significantly reduced by an order of magnitude.

## 5 IMPLEMENTATION DETAILS

We provide more experimental details on the five datasets: *Digits* [71], *CIFAR-10-C* [22], *SYTHIA* [54], *Amazon Reviews* [6],

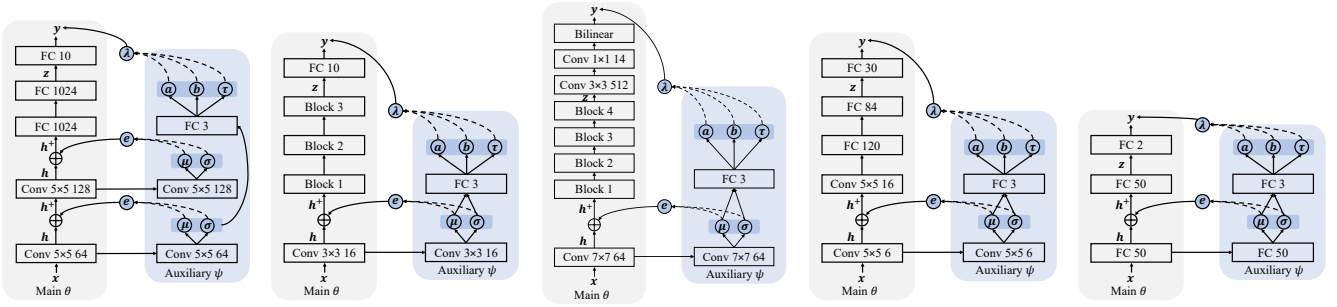


Fig. 5: Architectures of main and auxiliary models. **From left to right:** (a) *Digits* [71]; (b) *CIFAR-10-C* [22]; (c) *SYTHIA* [54]; (d) *Google Commands* [73], and (e) *Amazon Reviews* [6].

and *Google Commands* [73]. In learnable label mixup, we use Gaussian parameters of feature perturbations from the first layer. We choose specific backbone models, and design different auxiliary models as well as training strategies according to characteristics of each dataset.

In *Digits* [71], the backbone model is *conv-pool-conv-pool-fc-fc-softmax*. There are two  $5 \times 5$  convolutional layers with 64 and 128 channels respectively. Each convolutional layer is followed by a max pooling layer with the size of  $2 \times 2$ . The size of the two Fully-Connected (FC) layers is 1024 and the size of the softmax layer is 10. We inject perturbations to latent features of the two convolutional layers. The detailed architecture is presented in Fig. 5 (a). We employ Adam [27] for optimization with batch size of 32. We train for total 10K iterations with learning rate of  $10^{-4}$ .

In *CIFAR-10-C* [22], we evaluate our method on two backbones: AllConvNet (AllConv) [56] and Wide Residual Network (WRN) [76] with 40 layers and the width of 2. In AllConv [56], the model starts with three  $3 \times 3$  convolutional layers with 96 channels. Each layer is followed by batch normalization (BN) [26] and GELU. They convert the original image with three channels to feature maps of 96 channels. Then, the features go through three  $3 \times 3$  convolutional layers with 192 channels. After that, the features are fed into two  $1 \times 1$  convolutional layers with 192 channels and an average pooling layer with the size of  $8 \times 8$ . Finally, a softmax layer with the size of 10 is used for classification. In WRN [76]. The first layer is a  $3 \times 3$  convolutional layer. It converts the original image with three channels to feature maps of 16 channels. Then the features go through three blocks of  $3 \times 3$  convolutional layers. Each block consists of six basic blocks and each basic block is composed of two convolutional layers with the same number of channels. And their channels are  $\{32, 64, 128\}$  respectively. Each layer is followed by batch normalization (BN) [26]. An average pooling layer with the size of  $8 \times 8$  is appended to the output of the third block. Finally, a softmax layer with the size of 10 is used for prediction. In both AllConv [56] and WRN [76], we only inject perturbations to the latent features of the first convolutional layer. We also tried to inject perturbations in the next few layers or groups, however, we found the performance degraded severely mainly due to its large effect on the semantic feature, *i.e.*, outputs before the activation layer. The detailed architecture with backbone of WRN is shown in Fig. 5 (b). Following the training procedure in [76],

we use SGD with Nesterov momentum and set the batch size to 128. The initial learning rate is 0.1 with a linear decay and the number of epochs is 200.

In *SYTHIA* [54], we use FCN-32s [41] with the backbone of ResNet-50 [21]. The model consists of a feature extractor and a classifier. We use ResNet-50 [21] as the feature extractor, which is composed of a  $7 \times 7$  convolutional layer with 64 channels and four convolutional blocks. The classifier consists of a  $3 \times 3$  convolutional layer with 512 channels, a  $1 \times 1$  convolutional layer with 14 channels, and a bilinear layer used to up-sample the coarse outputs to the original size. We use Adam with the learning rate  $\alpha = 0.0001$ . We set the batch size to 8 and the number of epochs to 50.

In *Amazon Reviews* [6], the extracted features are fed into two FC layers with the size of 50. A softmax layer with the size of two is used to classify the sentiment of reviews into “positive” or “negative”. All models are trained using Adam [27] optimizer with learning rate of  $10^{-4}$  and batch size of 32 for 1000 iterations. In *Google Commands* [73], the mel-spectrogram features are fed into LeNet [33] as one-channel input. The original image is fed into two  $5 \times 5$  convolutional layers with the channels of 6 and 16, respectively. Next, the features go through two FC layers with the size of 120 and 84, respectively. Finally, a softmax layer with the size of 30 is leveraged to predict the spoken word. Models are trained using Adam [27] with learning rate  $10^{-4}$  and batch size of 128 for 30 epochs. For the corrupted test sets, the range of “amplitude change” is (0.7, 1.1). The maximum scales of “pitch change”, “background noise”, and “stretch” are 0.2, 0.45, and 0.2, respectively. The maximum shift of “time shift” is 8. In the experiments of *Amazon Reviews* [6] and *Google Commands* [73], feature perturbations are appended to the first layer. The detailed architectures used for *Google Commands* [73] and *Amazon Reviews* [6] are presented in Fig. 5 (c) and (d), respectively.

## 6 EXPERIMENTS

To best validate the performance, we conduct a series of experiments to compare our approach with existing methods that can be roughly grouped in four categories: **1) Adversarial training:** PAR [72], Self-super [23], and PGD [43]. **2) Data augmentation:** Mixup [77], JiGen [5], Cutout [9], and AutoAug [7]. **3) Domain adaptation:** DIRT [60], SE [13], SBADA [55], FADA [47], and CCSA [48].

**4) Domain generalization:** ERM [30], GUD [71], and M-ADA [52]. The experimental results prove that our method achieves superior performance on a wide scope of tasks, including *image classification* [22], *semantic segmentation* [54], *text classification* [6], and *speech recognition* [73].

## 6.1 Image Classification

In this section, we perform experiments on *Digits* [71] and *CIFAR-10-C* [22] for image classification. We report the results of classification accuracy, uncertainty estimation and few-shot domain adaptation.

**Datasets.** We validate our method on the following two benchmark datasets for image classification. (1) *Digits* is used for digit classification and consists of five sub-datasets: MNIST [34], MNIST-M [14], SVHN [51], SYN [14], and USPS [8]. Each sub-dataset can be viewed as a different domain. Each image in these datasets contains one single digit with different styles and backgrounds. (2) *CIFAR-10-C* [22] is a robustness benchmark consisting of 19 corruptions types with five levels of severity applied to the test set of CIFAR-10 [31]. The corruptions consist of four main categories: noise, blur, weather, and digital. Each corruption has five-level severities and “5” indicates the most corrupted one.

**Setup.** *Digits*: following the experimental setup in [71], we use 10,000 samples in the training set of MNIST for training, and evaluate models on the other four sub-datasets. We use a ConvNet [32] with architecture *conv-pool-conv-pool-fc-fc-softmax* as the backbone. All images are resized to  $32 \times 32$ , and the channels of MNIST and USPS are duplicated to make them as RGB images. We employ Adam [27] for optimization with batch size of 32. We train for total 10K iterations with learning rate of  $10^{-4}$ . *CIFAR-10-C*: we train models on CIFAR-10 and evaluate them on CIFAR-10-C. Following the setting of [24], we evaluate the model on 15 corruptions. We train models on AllConvNet (AllConv) [56] and Wide Residual Network (WRN) [76] with 40 layers and the width of 2. Following the training procedure in [76], we use SGD with Nesterov momentum and set the batch size to 128. The initial learning rate is 0.1 with a linear decay and the number of epochs is 100.

**Results. 1) Classification accuracy.** Tab. 1 shows the classification results of *Digits* and *CIFAR-10-C*. On the experiment of *Digits*, GUD [71], M-ADA [52], and our method outperform all baselines of the second block. And our method outperforms M-ADA [52] on *SYN* and the average accuracy by 8.1% and 1.8%, respectively. On the experiment of *CIFAR-10-C*, our method consistently outperforms all baselines on two different backbones, suggesting its strong generalization on various image corruptions. The classification results on corruptions across five levels of severity are shown in Fig. 7. As seen, our method outperforms other methods across all levels of corruption severity. Specifically, the gap between M-ADA [52] (previous SOTA) and our method gets larger with the level of severity increasing. Fig. 6 shows more detailed comparisons of all corruptions at the highest level of severity. As seen, our method achieves substantial gains across a wide variety of corruptions, with a small drop of performance in only two corruption types: brightness and contrast. Especially, accuracies are significantly improved

TABLE 2: Few-shot domain adaptation accuracy (%) on *MNIST(M)*, *USPS(U)*, and *SVHN(S)*.  $|T|$  denotes the number of target samples (per class) used during model training. Our method achieves the best performance on the average of  $U \rightarrow M$ ,  $M \rightarrow S$ , and  $S \rightarrow M$ . The result on the hardest task ( $M \rightarrow S$ ) is even competitive to that of SBADA [55] which takes advantage of all images of the target domain for training.

Method	$ T $	U $\rightarrow$ M	M $\rightarrow$ S	S $\rightarrow$ M	Avg.
DIRT-T [60]		-	54.50	<b>99.40</b>	-
SE [13]	All	<b>98.07</b>	13.96	99.18	70.40
SBADA [55]		97.60	<b>61.08</b>	76.14	78.27
FADA [47]	7	91.50	47.00	87.20	75.23
CCSA [48]	10	95.71	37.63	94.57	75.97
<b>Ours</b>	7	92.97	58.12	89.30	80.13
	10	93.16	59.77	91.67	<b>81.53</b>

by 20% on corruptions of noise. The results demonstrate its strong generalization capability on severe corruptions. **2) Uncertainty estimation.** We compare the proposed *domain uncertainty score* (Sec.4.3) with a more time-consuming one based on Bayesian models [4]. The former computes the uncertainty through one-pass forwarding, while the latter computes the variance of the output through repeated sampling of 30 times. Fig. 8 show the results of uncertainty estimation on *Digits* and *CIFAR-10-C*. As seen, our estimation shows consistent results with Bayesian uncertainty estimation on both *Digits* and *CIFAR-10-C*, suggesting its high efficiency. **3) Few-shot domain adaptation.** Although our method is designed for single domain generalization, we also show that our method can be easily applied for few-shot domain adaptation [47] due to the meta-learning training scheme. Following the setup in [52], the model is first pre-trained on the source domain  $\mathcal{S}$  and then fine-tuned on the target domain  $\mathcal{T}$ . We conduct three few-shot domain adaption tasks: *USPS(U)  $\rightarrow$  MNIST(M)*, *MNIST(M)  $\rightarrow$  SVHN(S)*, and *SVHN(S)  $\rightarrow$  MNIST(M)*. Results of the three tasks are shown in Tab. 2. Our method achieves the best performance on the average of three tasks. The result on the hardest task ( $M \rightarrow S$ ) is even competitive to that of SBADA [55] which takes advantage of all unlabelled images of the target domain for training.

## 6.2 Semantic Segmentation

In this section, we perform experiments on *SYTHIA* [54] for semantic segmentation. We report the results of the mean Intersection Over Union (mIoU) and visual comparison.

**Datasets.** *SYTHIA* [54] is a synthetic dataset of urban scenes, used for semantic segmentation in the context of driving scenarios. This dataset consists of photo-realistic frames rendered from virtual cities and comes with precise pixel-level semantic annotations. It is composed of the same traffic situation but under different locations (Highway, New York-like City, and Old European Town are selected) and different weather/illumination/season conditions (Dawn, Fog, Night, Spring, and Winter are selected).

**Setup.** In this experiment, Highway is the source domain, and New York-like City together with Old European Town are unseen domains. Following the protocol in [52], [71],



Domain	Mixup [77]	PAR [72]	Self-super [23]	JiGen [5]	ERM [30]	GUD [71]	M-ADA [52]	Ours
SVHN [34]	28.5	30.5	30.0	33.8	27.8	35.5	<u>42.6</u>	<b>43.3</b>
MNIST-M [14]	54.0	58.4	58.1	57.8	52.8	60.4	<b>67.9</b>	<u>67.4</u>
SYN [14]	41.2	44.1	41.9	43.8	39.9	45.3	<u>49.0</u>	<b>57.1</b>
USPS [8]	76.6	76.9	77.1	77.2	76.5	77.3	<b>78.5</b>	<u>77.4</u>
Avg.	50.1	52.5	51.8	53.1	49.3	54.6	<u>59.5</u>	<b>61.3</b>

Model	Mixup [77]	Cutout [9]	AutoAug [7]	PGD [43]	ERM [30]	GUD [71]	M-ADA [52]	Ours
AllConv [56]	75.4	67.1	70.8	71.9	69.2	73.6	<u>75.9</u>	<b>79.6</b>
WRN [76]	77.7	73.2	76.1	73.8	73.1	75.3	<u>80.2</u>	<b>83.4</b>

TABLE 1: Image classification accuracy (%) on *Digits* [71] (**top**) and *CIFAR-10-C* [22] (**bottom**). We compare with *robust training* (**Columns 1-4**) and *domain generalization* (**Columns 5-7**). For *Digits*, all models are trained on *MNIST* [34]. For *CIFAR-10-C*, two widely employed backbones are evaluated. Our method outperforms M-ADA [52] (previous SOTA) consistently in all settings.

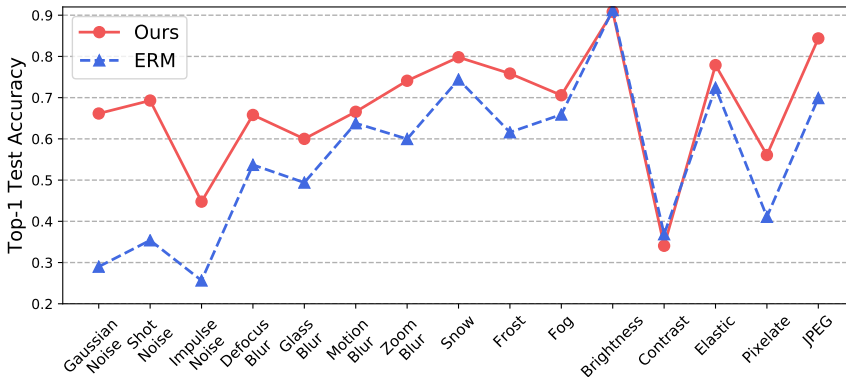


Fig. 6: Classification accuracy on fifteen corruptions of *CIFAR-10-C* using the backbone of WRN (40-2). Following Fig. 7, the accuracy of each corruption with the highest level of severity is presented. Our method achieves 20% improvements on corruptions of noise.

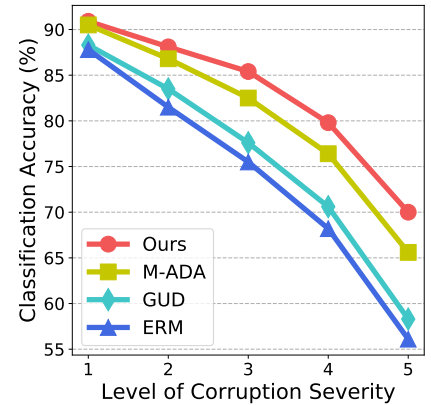


Fig. 7: Classification accuracy (%) on five levels of corruption severity. Our method has the smallest degradation under the highest level of corruption severity.

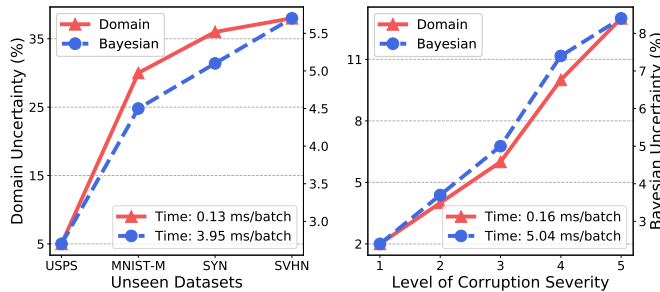


Fig. 8: Uncertainty estimation on *Digits* (**left**) and *CIFAR-10-C* (**right**). Our prediction of *domain uncertainty* is consistent with *Bayesian uncertainty*, while our method is an order of magnitude faster since we forward data only once.

we only use the images from the left front camera and 900 images are randomly sample from each source domain. We use FCN-32s [41] with the backbone of ResNet-50 [21].

**Results.** We report the mean Intersection Over Union (mIoU) of *SYTHIA* in Tab. 3. As can be observed, our method outperforms previous SOTA in most unseen environments. Visual comparison on *SYTHIA* [54] is shown in Fig. 9. Results demonstrate that our model can better generalize to the

changes of locations, weather, and time.

### 6.3 Text Classification

In this section, we perform experiments on *Amazon Reviews* [6] for text classification.

**Datasets.** *Amazon Reviews* [6] contains reviews of products belonging to four categories - books(b), DVD(d), electronics(e) and kitchen appliances(k). The difference in textual description of the four product categories manifests as domain shift. Following [9], we use unigrams and bigrams as features resulting in 5000 dimensional vector representations. The reviews are assigned binary labels - 0 if the rating of the product is up to 3 stars, and 1 if the rating is 4 or 5 stars.

**Setup.** We train the models on one source domain (books or dvd), and evaluate them on the other three domains. Similar to [14], we use a neural network with two hidden layers (both with 50 neurons) as the backbone. All models are trained using Adam [27] optimizer with learning rate of  $10^{-4}$  and batch size of 32 for 1000 iterations.

**Results.** Tab. 4 shows the results of text classification on *Amazon Reviews* [6]. We found that our method outperform previous ones on all the three unseen domains when the source domain is “books” or “kitchen”. Specially, our method outperforms ERM [30] by 3.5% on “books → electronics”.

Source Domain	Method	New York-like City					Old European Town					Avg.
		Dawn	Fog	Night	Spring	Winter	Dawn	Fog	Night	Spring	Winter	
Highway/Dawn	ERM [30]	27.8	2.7	0.9	6.8	1.7	52.8	31.4	15.9	33.8	13.4	18.7
	GUD [71]	27.1	4.1	1.6	7.2	2.8	52.8	34.4	18.2	33.6	14.7	19.7
	M-ADA [52]	<u>29.1</u>	<u>4.4</u>	<u>4.8</u>	<u>14.1</u>	<u>5.0</u>	<u>54.3</u>	<u>36.0</u>	<u>23.2</u>	<u>37.5</u>	<u>14.9</u>	<u>22.3</u>
	<b>Ours</b>	<b>29.3</b>	<b>7.6</b>	<b>2.8</b>	<b>12.7</b>	<b>10.2</b>	<b>54.9</b>	<b>37.0</b>	<b>25.3</b>	<b>37.2</b>	<b>17.7</b>	<b>23.5</b>
Highway/Fog	ERM [30]	17.2	34.8	12.4	26.4	11.8	33.7	55.0	26.2	41.7	12.3	27.2
	GUD [71]	18.8	35.6	12.8	26.0	13.1	37.3	56.7	28.1	43.6	13.6	28.5
	M-ADA [52]	<u>21.7</u>	32.0	9.7	<u>26.4</u>	<u>13.3</u>	<u>42.8</u>	56.6	<b>31.8</b>	42.8	12.9	<u>29.0</u>
	<b>Ours</b>	<b>23.0</b>	<b>36.2</b>	<b>13.5</b>	<b>27.6</b>	<b>14.2</b>	<b>43.1</b>	<b>57.4</b>	<u>31.0</u>	<b>44.6</b>	<u>13.1</u>	<b>30.4</b>

TABLE 3: Semantic segmentation mIoU (%) on SYNTHIA [54]. All models are trained on the single source from Highway and evaluated on unseen environments from New York-like City and Old European Town.

Method	books			dvd			kitchen			electronics		
	d	k	e	b	k	e	b	d	e	b	d	k
ERM [30]	78.7	74.6	63.6	78.5	82.1	<b>75.2</b>	<u>75.4</u>	76.0	81.2	<u>69.4</u>	<b>74.8</b>	83.9
GUD [71]	79.1	75.6	64.7	78.1	82.0	74.6	<u>74.9</u>	76.7	81.6	<u>68.9</u>	74.2	84.4
M-ADA [52]	<u>79.4</u>	<u>76.1</u>	<u>65.3</u>	<u>78.8</u>	<u>82.6</u>	74.3	75.2	<u>77.3</u>	<u>82.3</u>	69.0	73.7	<u>84.8</u>
<b>Ours</b>	<b>80.2</b>	<b>76.8</b>	<b>67.1</b>	<b>80.1</b>	<b>83.5</b>	<u>75.0</u>	<b>76.1</b>	<b>78.2</b>	<b>83.5</b>	<b>70.2</b>	<u>74.5</u>	<b>85.7</b>

TABLE 4: Text classification accuracy (%) on Amazon Reviews [6]. Models are trained on one text domain and evaluated on unseen text domains. Our method outperforms others in all settings except “dvd → electronics” and “electronics → dvd”. The possible reason is that “dvd” and “electronics” may share a similar distribution while our method creates large distribution shift.

Method	Time		Frequency		
	Amp.	Pit.	Noise	Stretch	Shift
ERM [30]	63.8	71.6	73.9	72.9	70.5
GUD [71]	64.1	<u>72.1</u>	74.8	73.1	70.9
M-ADA [52]	<u>64.5</u>	71.9	<u>75.4</u>	<u>73.8</u>	<u>71.4</u>
<b>Ours</b>	<b>65.3</b>	<b>73.5</b>	<b>75.8</b>	<b>75.0</b>	<b>72.5</b>

TABLE 5: Speech recognition accuracy (%) on Google Commands [73]. Models are trained on clean set and evaluated on five corrupted sets. Results validate our strong generalization on corruptions in both time and frequency domains.

We observe that there is a little drop in accuracy on “dvd → electronics” and “electronics → dvd”. One possible reason is that “electronics” and “dvd” may share a similar distribution. And our method creates large distribution shift, degrading the performance on them.

### 6.4 Speech Recognition

In this section, we perform experiments on Google Commands [73] for speech recognition.

**Datasets.** Google Commands [73] contains 65000 utterances (one second long) from thousands of people. The goal is to classify them to 30 command words. There are 56196, 7477, and 6835 examples for training, validation, and test. To simulate domain shift in real-world scenario, we apply five common corruptions in both time and frequency domains. This creates five test sets that are “harder” than training sets, namely amplitude change (Amp.), pitch change (Pit.), background noise (Noise), stretch (Stretch), and time shift (Shift).

In detail, the range of “amplitude change” is (0.7,1.1). The maximum scales of “pitch change”, “background noise”, and “stretch” are 0.2, 0.45, and 0.2, respectively. The maximum shift of “time shift” is 8.

**Setup.** We train the models on the clean train set, and evaluate them on the corrupted test sets. We encode each audio into a mel-spectrogram with the size of 1x32x32 and feed them to LeNet [33] as one-channel input. All models are trained using Adam optimizer [27] with learning rate  $10^{-4}$  and batch size of 128 for 30 epoches.

**Results.** Tab. 5 shows the results of speech recognition on Google Commands [73]. Our method outperforms the other three methods on all the five corrupted test sets, indicating its strong generalization ability in both time and frequency domain. In detail, our method outperforms the second best by 0.8% on “amplitude change”, 1.4% on “pitch change”, 0.4% on “background noise”, 1.2% on “stretch”, and 1.1% on “time shift”, respectively. We can see that the improvements on “pitch change”, “stretch”, and “time shift” are more significant than those on “amplitude change” and “background noise”.

### 6.5 Ablation Study

We have shown that our method yields significant improvements on five datasets across image, text, and speech. In this section, we perform ablation study to investigate key components of our method. For Digits [71], we report the average performance of all unseen domains. For CIFAR-10-C [22], we report the average performance of all types of corruptions at the highest level of severity.

**Uncertainty assessment.** We visualize feature perturbation  $|e| = |h^+ - h|$  and the embedding of domains at different

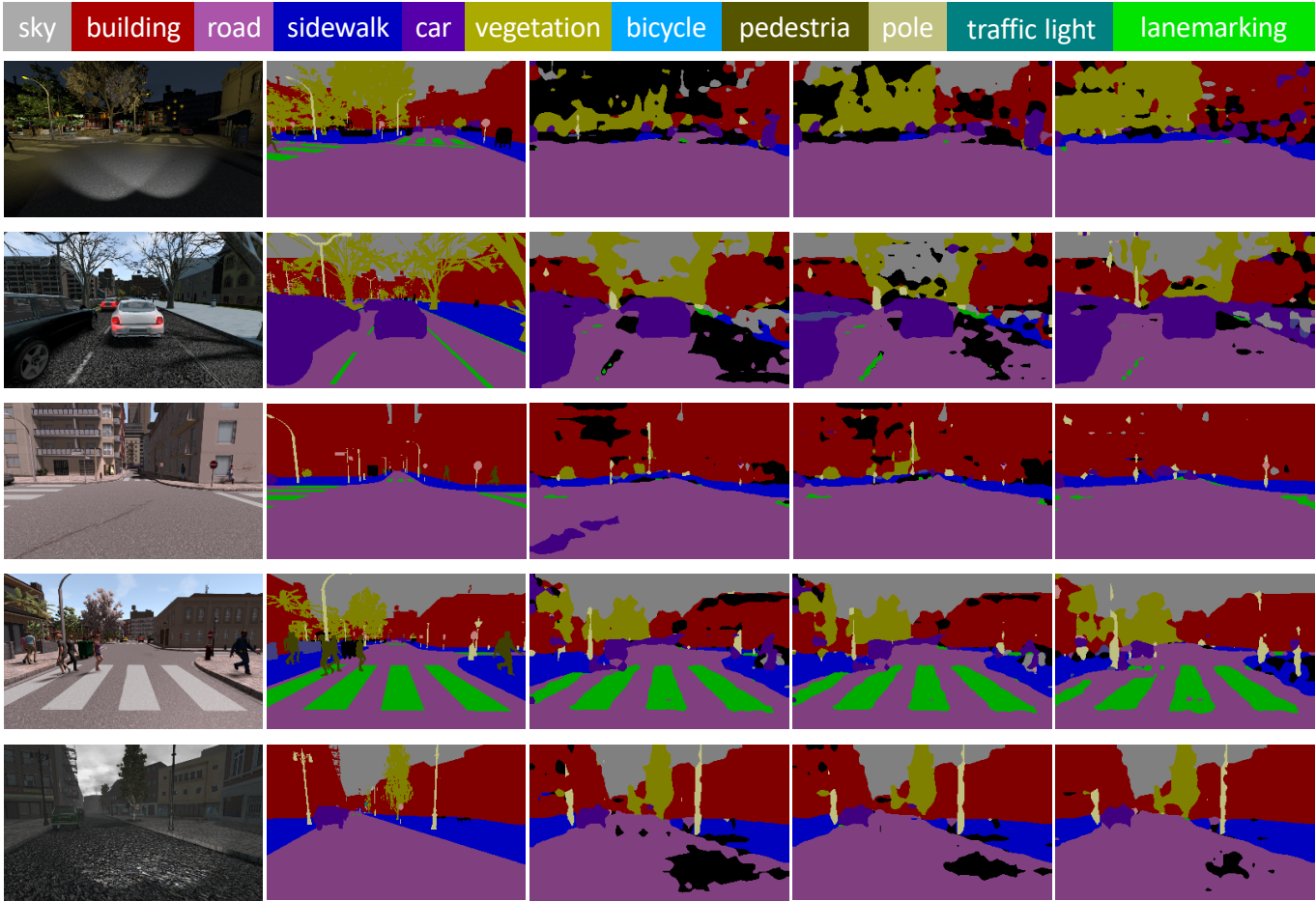


Fig. 9: Examples of semantic segmentation on SYTHIA [54]. **From left to right:** (a) images from unseen domains; (b) ground truth; (c) results of ERM [30]; (d) results of M-ADA [52]; and (e) results of our method. Best viewed in color and zoom in for details.

	Digits [71]	CIFAR-10-C [22]
<b>Full Model</b>	<b>61.3±0.73</b>	<b>70.2±0.62</b>
Random Gaussian	51.0±0.36	64.0±0.18
Determ. perturb.	59.7±0.70	67.0±0.57
Random $\mu$	60.5±0.75	69.1±0.61
Random $\sigma$	60.7±0.65	69.5±0.60

TABLE 6: Ablation study of feature perturbation.

training iterations  $T$  on MNIST [34]. We use t-SNE [42] to visualize the source and augmented domains without and with uncertainty assessment in the embedding space. Results are shown in Fig. 10. In the model without uncertainty (left), the feature perturbation  $e$  is sampled from  $\mathcal{N}(\mathbf{0}, \mathbf{I})$  without learnable parameters. In the model with uncertainty (right), we observe that most perturbations are located in the background area which increases the variation of  $S^+$  while keeping the category unchanged. As a result, models with uncertainty can create large domain transportation in a curriculum learning scheme, yielding safe augmentation and improved accuracy on unseen domains. We visualize the density of  $y^+$  in Fig. 11. As seen, models with uncertainty

can significantly augment the label space.

**Variational feature perturbation.** We investigate different designs of feature perturbation: 1) *Random Gaussian*: the feature perturbation  $e$  is sampled from  $\mathcal{N}(\mathbf{0}, \mathbf{I})$  without learnable parameters. 2) *Deterministic perturbation*: we directly add the learned  $\mu$  to  $h$  without sampling, yielding  $h^+ \leftarrow h + \text{Softplus}(\mu)$ . 3) *Random  $\mu$* : the feature perturbation  $e$  is sampled from  $\mathcal{N}(\mathbf{0}, \sigma)$ , where  $\mu = \mathbf{0}$ . 4) *Random  $\sigma$* :  $e$  is sampled from  $\mathcal{N}(\mu, \mathbf{I})$ , where  $\sigma = \mathbf{I}$ . Results on these different choices are shown in Tab. 6. As seen, *Random Gaussian* yields the lowest accuracy on both datasets, indicating the necessity of learnable perturbations. *Deterministic perturbation* is inferior to *Random  $\mu$*  and *Random  $\sigma$* , suggesting that sampling-based perturbation can effectively increase the domain capacity. Finally, either *Random  $\mu$*  or *Random  $\sigma$*  is slightly worse than the full model. We conclude that both learnable  $\mu$  and  $\sigma$  contribute to the final performance.

**Learnable label space mixup.** We implement two variants of label space *mixup*: 1) *Without mixup*: the model is trained without label augmentation. 2) *Random mixup*: the mixup coefficient  $\lambda$  is sampled from a fixed distribution  $\text{Beta}(1, 1)$ . Results on the two variants are reported in Tab. 7. We notice that *Random mixup* achieves better performance than *without mixup*. The results support our claim that label

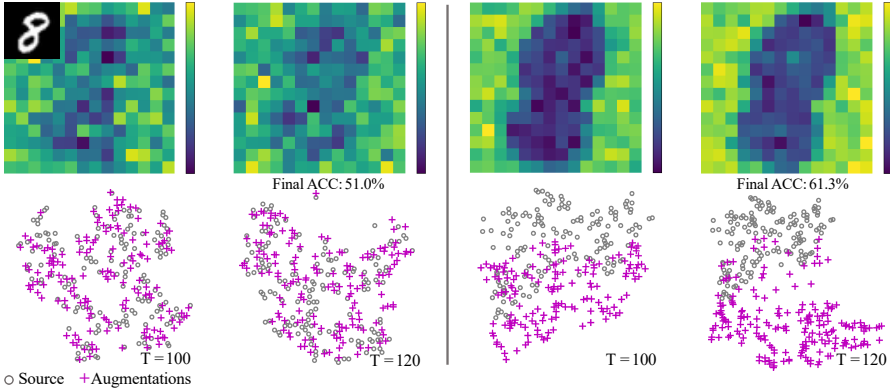


Fig. 10: Visualization of feature perturbation  $|e| = |h^+ - h|$  (Top) and embedding of domains (Bottom) at different training iterations  $T$  on *MNIST*. Left: Models w/o uncertainty; Right: Models w/ uncertainty. Most perturbations are located in the background area and models w/ uncertainty can create large domain transportation in a curriculum learning scheme.

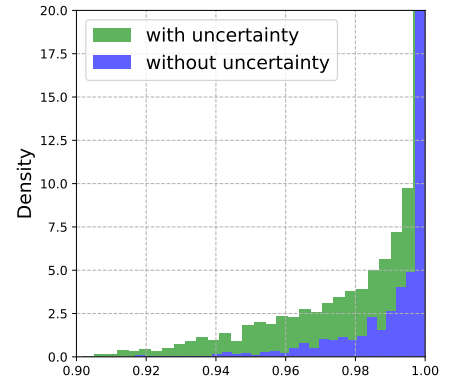


Fig. 11: Visualization of label mixup  $y^+$  on *MNIST*. Models w/ uncertainty can encourage more smoothing labels and significantly increase the capacity of label space.

	Digits [71]	CIFAR-10-C [22]
<b>Full Model</b>	<b>61.3±0.73</b>	<b>70.2±0.62</b>
w/o mixup	60.6±0.76	67.4±0.64
Random mixup	60.9±1.10	69.4±0.58

TABLE 7: Ablation study of label space mixup.

	Digits [71]	CIFAR-10-C [22]
<b>Full Model</b>	<b>61.3±0.73</b>	<b>70.2±0.62</b>
w/o adv. training	51.8±0.71	60.0±0.55
w/o relaxation $W_p$	60.9±0.79	69.0±0.59
w/o minimizing $\phi_p$	60.6±0.91	69.6±0.75

TABLE 8: Ablation study of training strategy.

augmentation can further improve the model performance. The learnable mixup (full model) achieves the best results, suggesting that the proposed learning label space mixup can create informative domain interpolations for robust learning.

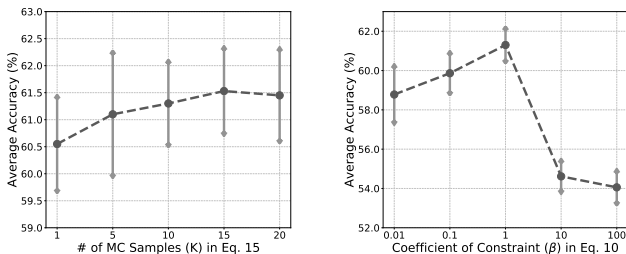


Fig. 12: Ablation study on hyper-parameters  $K$  and  $\beta$ . The average accuracy on the four unseen domains (*MNIST-M* [14], *SVHN* [51], *SYN* [14], and *USPS* [8]) is presented. We set  $K = 15$  and  $\beta = 1$  according to the best classification accuracy.

**Training strategy.** At last, we compare different training strategies. 1) *Without adversarial training*: models are learned

without adversarial training (Eq. 10). 2) *Without meta-learning*: the source  $\mathcal{S}$  and augmentations  $\mathcal{S}^+$  are trained together without the meta-learning scheme. 3) *Without minimizing  $\phi_p$* :  $\phi_p$  is not optimized in Eq. 15. Results are reported in Tab. 8. The adversarial training contributes most to the improvements: 9.5% on *Digits* and 10.2% on *CIFAR-10-C*. Meta-learning consistently improve the accuracy and reduce the deviation on both datasets. We notice that the accuracy is slightly dropped without minimization of  $\phi_p$ , possibly due to the excessive accumulation of perturbations.

**Hyper-parameter tuning of  $K$  and  $\beta$ .** We study the effect of two important hyper-parameters of our model: the number of Monte-Carlo (MC) samples ( $K$ ) and the coefficient of constraint ( $\beta$ ). We report the average accuracy on the four unseen domains (*MNIST-M* [14], *SVHN* [51], *SYN* [14], and *USPS* [8]). We present the classification results under different hyper-parameters in Fig. 12.

**1) Number of MC samples ( $K$ ).** The classification accuracy on *Digits* [71] with different  $K$  is shown in Fig. 12 (a). We notice that the average accuracy gradually increases from  $K = 1$  to  $K = 15$  and remains stable when  $K = 20$ .

**2) Coefficient of constraint ( $\beta$ ).** The constraint is used to make adversarial domain augmentation satisfy the worst-case constraint. Results on *Digits* [71] with different  $\beta$  is presented in Fig. 12 (b). As seen, the accuracy falls dramatically when  $\beta = 10$ , because large  $\beta$  may severely limit the domain transportation and create domain augmentations similar to the source.

## 7 CONCLUSION

In this work, we introduced uncertain out-of-domain generalization to tackle the problem of single source generalization. Our method explicitly model the uncertainty of domain augmentations in both input and label spaces. In input space, the proposed uncertainty-guided feature perturbation resolves the limitation of raw data augmentation, yielding a domain-knowledge-free solution for various modalities. In label space, the proposed uncertainty-guided label mixup further increases the domain capacity. The proposed *domain uncertainty score* is capable of estimating uncertainty with

high efficiency, which plays a crucial role for safe deployment. Finally, the proposed Bayesian meta-learning framework can maximize the posterior distribution of domain augmentations, such that the learned model can generalize well on unseen domains. The experimental results prove that our method achieves superior performance on a wide scope of tasks, including *image classification*, *semantic segmentation*, *text classification*, and *speech recognition*. In addition to the superior performances we achieved through these experiments, a series of ablation studies further validate the effectiveness of key components in our method. In the future, we expect to extend our work to semi-supervised learning or knowledge transferring in multimodal learning.

## REFERENCES

- [1] M. Andrychowicz, M. Denil, S. Gómez, M. W. Hoffman, D. Pfau, T. Schaul, B. Shillingford, and N. de Freitas. Learning to Learn by Gradient Descent by Gradient Descent. In *Annual Conference on Neural Information Processing Systems*, pages 3981–3989, 2016.
- [2] Y. Balaji, S. Sankaranarayanan, and R. Chellappa. Metareg: Towards domain generalization using meta-regularization. In *Annual Conference on Neural Information Processing Systems*, pages 998–1008, 2018.
- [3] Y. Bengio, J. Louradour, R. Collobert, and J. Weston. Curriculum learning. In *International Conference on Machine Learning*, pages 41–48, 2009.
- [4] C. Blundell, J. Cornebise, K. Kavukcuoglu, and D. Wierstra. Weight uncertainty in neural network. In *International Conference on Machine Learning*, pages 1613–1622, 2015.
- [5] F. M. Carlucci, A. D’Innocente, S. Bucci, B. Caputo, and T. Tommasi. Domain generalization by solving jigsaw puzzles. In *Proceedings of the IEEE/CVF Conference on Computer Vision and Pattern Recognition*, pages 2229–2238, 2019.
- [6] M. Chen, Z. Xu, K. Q. Weinberger, and F. Sha. Marginalized denoising autoencoders for domain adaptation. In *International Conference on Machine Learning*, pages 1627–1634, 2012.
- [7] E. D. Cubuk, B. Zoph, D. Mane, V. Vasudevan, and Q. V. Le. Autoaugment: Learning augmentation strategies from data. In *Proceedings of the IEEE/CVF Conference on Computer Vision and Pattern Recognition*, pages 113–123, 2019.
- [8] J. S. Denker, W. Gardner, H. P. Graf, D. Henderson, R. E. Howard, W. Hubbard, L. D. Jackel, H. S. Baird, and I. Guyon. Neural network recognizer for hand-written zip code digits. In *Annual Conference on Neural Information Processing Systems*, pages 323–331, 1989.
- [9] T. DeVries and G. W. Taylor. Improved regularization of convolutional neural networks with cutout. *arXiv preprint arXiv:1708.04552*, 2017.
- [10] Q. Dou, D. C. de Castro, K. Kamnitsas, and B. Glocker. Domain generalization via model-agnostic learning of semantic features. In *Annual Conference on Neural Information Processing Systems*, pages 6447–6458, 2019.
- [11] C. Finn, P. Abbeel, and S. Levine. Model-agnostic meta-learning for fast adaptation of deep networks. In *International Conference on Machine Learning*, pages 1126–1135, 2017.
- [12] C. Finn, K. Xu, and S. Levine. Probabilistic model-agnostic meta-learning. In *Annual Conference on Neural Information Processing Systems*, pages 9516–9527, 2018.
- [13] G. French, M. Mackiewicz, and M. Fisher. Self-ensembling for visual domain adaptation. In *International Conference on Learning Representations*, 2018.
- [14] Y. Ganin and V. Lempitsky. Unsupervised Domain Adaptation by Backpropagation. In *International Conference on Machine Learning*, pages 1180–1189, 2015.
- [15] M. Ghifary, W. Bastiaan Kleijn, M. Zhang, and D. Balduzzi. Domain generalization for object recognition with multi-task autoencoders. In *Proceedings of the IEEE/CVF International Conference on Computer Vision*, pages 2551–2559, 2015.
- [16] I. Goodfellow, J. Pouget-Abadie, M. Mirza, B. Xu, D. Warde-Farley, S. Ozair, A. Courville, and Y. Bengio. Generative adversarial nets. In *Annual Conference on Neural Information Processing Systems*, pages 2672–2680, 2014.
- [17] I. J. Goodfellow, J. Shlens, and C. Szegedy. Explaining and harnessing adversarial examples. In *International Conference on Learning Representations*, 2015.
- [18] E. Grant, C. Finn, S. Levine, T. Darrell, and T. Griffiths. Recasting gradient-based meta-learning as hierarchical bayes. In *International Conference on Learning Representations*, 2018.
- [19] A. Graves. Practical variational inference for neural networks. In *Annual Conference on Neural Information Processing Systems*, pages 2348–2356, 2011.
- [20] T. Grubinger, A. Birlutiu, H. Schöner, T. Natschläger, and T. Heskes. Multi-domain transfer component analysis for domain generalization. *Neural Processing Letters (NPL)*, 46(3):845–855, 2017.
- [21] K. He, X. Zhang, S. Ren, and J. Sun. Deep Residual Learning for Image Recognition. In *Proceedings of the IEEE/CVF Conference on Computer Vision and Pattern Recognition*, pages 770–778, 2016.
- [22] D. Hendrycks and T. Dietterich. Benchmarking neural network robustness to common corruptions and perturbations. *International Conference on Learning Representations*, 2019.
- [23] D. Hendrycks, M. Mazeika, S. Kadavath, and D. Song. Using self-supervised learning can improve model robustness and uncertainty. In *Annual Conference on Neural Information Processing Systems*, pages 15637–15648, 2019.
- [24] D. Hendrycks, N. Mu, E. D. Cubuk, B. Zoph, J. Gilmer, and B. Lakshminarayanan. Augmix: A simple data processing method to improve robustness and uncertainty. In *International Conference on Learning Representations*, 2020.
- [25] G. E. Hinton and D. Van Camp. Keeping the neural networks simple by minimizing the description length of the weights. In *Proceedings of the Sixth Annual ACM Conference on Computational Learning Theory*, pages 5–13, 1993.
- [26] S. Ioffe and C. Szegedy. Batch normalization: Accelerating deep network training by reducing internal covariate shift. In *International Conference on Machine Learning*, pages 448–456, 2015.
- [27] D. P. Kingma and J. Ba. Adam: A Method for Stochastic Optimization. In *arXiv:1412.6980 [cs.LG]*, 2014.
- [28] D. P. Kingma and M. Welling. Auto-encoding variational bayes. In *International Conference on Learning Representations*, 2014.
- [29] G. Koch, R. Zemel, and R. Salakhutdinov. Siamese neural networks for one-shot image recognition. In *ICML Deep Learning Workshop*, 2015.
- [30] V. Koltchinskii. *Oracle Inequalities in Empirical Risk Minimization and Sparse Recovery Problems: Ecole d’Eté de Probabilités de Saint-Flour XXXVIII-2008*, volume 2033. Springer Science & Business Media, 2011.
- [31] A. Krizhevsky, G. Hinton, et al. Learning multiple layers of features from tiny images. 2009.
- [32] Y. LeCun, B. Boser, J. S. Denker, D. Henderson, R. E. Howard, W. Hubbard, and L. D. Jackel. Backpropagation applied to hand-written zip code recognition. *Neural Computation (NC)*, 1(4):541–551, 1989.
- [33] Y. Lecun, L. Bottou, Y. Bengio, and P. Haffner. Gradient-Based Learning Applied to Document Recognition. *Proceedings of the IEEE*, 86(11), 1998.
- [34] Y. LeCun, L. Bottou, Y. Bengio, and P. Haffner. Gradient-based learning applied to document recognition. *Proceedings of the IEEE*, 86(11):2278–2324, 1998.
- [35] H. B. Lee, H. Lee, D. Na, S. Kim, M. Park, E. Yang, and S. J. Hwang. Learning to balance: Bayesian meta-learning for imbalanced and out-of-distribution tasks. In *International Conference on Learning Representations*, 2020.
- [36] H. B. Lee, T. Nam, E. Yang, and S. J. Hwang. Meta dropout: Learning to perturb latent features for generalization. In *International Conference on Learning Representations*, 2019.
- [37] D. Li, Y. Yang, Y.-Z. Song, and T. M. Hospedales. Deeper, Broader and Artier Domain Generalization. In *Proceedings of the IEEE/CVF International Conference on Computer Vision*, pages 5542–5550, 2017.
- [38] D. Li, Y. Yang, Y.-Z. Song, and T. M. Hospedales. Learning to Generalize: Meta-Learning for Domain Generalization. In *Proceedings of the AAAI Conference on Artificial Intelligence*, pages 3490–3497, 2018.
- [39] K. Li and J. Malik. Learning to optimize. In *International Conference on Learning Representations*, 2017.
- [40] H. Liu, M. Long, J. Wang, and M. Jordan. Transferable adversarial training: A general approach to adapting deep classifiers. In *International Conference on Machine Learning*, pages 4013–4022, 2019.

- [41] J. Long, E. Shelhamer, and T. Darrell. Fully convolutional networks for semantic segmentation. In *Proceedings of the IEEE/CVF Conference on Computer Vision and Pattern Recognition*, pages 3431–3440, 2015.
- [42] L. v. d. Maaten and G. Hinton. Visualizing data using t-sne. *Journal of Machine Learning Research (JMLR)*, 9(Nov):2579–2605, 2008.
- [43] A. Madry, A. Makelov, L. Schmidt, D. Tsipras, and A. Vladu. Towards deep learning models resistant to adversarial attacks. In *International Conference on Learning Representations*, 2018.
- [44] M. Mancini, S. R. Bulò, B. Caputo, and E. Ricci. Best sources forward: domain generalization through source-specific nets. In *IEEE International Conference on Image Processing*, pages 1353–1357, 2018.
- [45] M. Mancini, S. R. Bulò, B. Caputo, and E. Ricci. Robust place categorization with deep domain generalization. *IEEE Robotics and Automation Letters (RAL)*, 3(3):2093–2100, 2018.
- [46] T. Miyato, S.-i. Maeda, M. Koyama, and S. Ishii. Virtual adversarial training: a regularization method for supervised and semi-supervised learning. *IEEE Transactions on Pattern Analysis and Machine Intelligence (TPAMI)*, 41(8):1979–1993, 2018.
- [47] S. Motiian, Q. Jones, S. Iranmanesh, and G. Doretto. Few-shot adversarial domain adaptation. In *Annual Conference on Neural Information Processing Systems*, pages 6670–6680, 2017.
- [48] S. Motiian, M. Piccirilli, D. A. Adjeroh, and G. Doretto. Unified Deep Supervised Domain Adaptation and Generalization. In *Proceedings of the IEEE/CVF International Conference on Computer Vision*, pages 5715–5725, 2017.
- [49] K. Muandet, D. Balduzzi, and B. Schölkopf. Domain Generalization via Invariant Feature Representation. In *International Conference on Machine Learning*, pages 10–18, 2013.
- [50] Z. Murez, S. Kolouri, D. Kriegman, R. Ramamoorthi, and K. Kim. Image to image translation for domain adaptation. In *Proceedings of the IEEE/CVF Conference on Computer Vision and Pattern Recognition*, pages 4500–4509, 2018.
- [51] Y. Netzer, T. Wang, A. Coates, A. Bissacco, B. Wu, and A. Y. Ng. Reading digits in natural images with unsupervised feature learning. In *NIPS Workshop on Deep Learning and Unsupervised Feature Learning*, 2011.
- [52] F. Qiao, L. Zhao, and X. Peng. Learning to learn single domain generalization. In *Proceedings of the IEEE/CVF Conference on Computer Vision and Pattern Recognition*, pages 12556–12565, 2020.
- [53] A. J. Ratner, H. Ehrenberg, Z. Hussain, J. Dunnmon, and C. Ré. Learning to Compose Domain-Specific Transformations for Data Augmentation. In *Annual Conference on Neural Information Processing Systems*, pages 3236–3246, 2017.
- [54] G. Ros, L. Sellart, J. Materzynska, D. Vazquez, and A. M. Lopez. The synthia dataset: A large collection of synthetic images for semantic segmentation of urban scenes. In *Proceedings of the IEEE/CVF Conference on Computer Vision and Pattern Recognition*, pages 3234–3243, 2016.
- [55] P. Russo, F. M. Carlucci, T. Tommasi, and B. Caputo. From source to target and back: symmetric bi-directional adaptive gan. In *Proceedings of the IEEE/CVF Conference on Computer Vision and Pattern Recognition*, pages 8099–8108, 2018.
- [56] T. Salimans and D. P. Kingma. Weight normalization: A simple reparameterization to accelerate training of deep neural networks. In *Annual Conference on Neural Information Processing Systems*, pages 901–909, 2016.
- [57] S. Sankaranarayanan, Y. Balaji, C. D. Castillo, and R. Chellappa. Generate to adapt: Aligning domains using generative adversarial networks. In *Proceedings of the IEEE/CVF Conference on Computer Vision and Pattern Recognition*, pages 8503–8512, 2018.
- [58] J. Schmidhuber. *Evolutionary principles in self-referential learning*. PhD thesis, Technische Universität München, 1987.
- [59] S. Shankar, V. Piratla, S. Chakrabarti, S. Chaudhuri, P. Jyothi, and S. Sarawagi. Generalizing Across Domains via Cross-Gradient Training. In *International Conference on Learning Representations*, 2018.
- [60] R. Shu, H. H. Bui, H. Narui, and S. Ermon. A dirt-t approach to unsupervised domain adaptation. In *International Conference on Learning Representations*, 2018.
- [61] A. Sinha, H. Namkoong, and J. Duchi. Certifying distributional robustness with principled adversarial training. In *International Conference on Learning Representations*, 2018.
- [62] J. Snell, K. Swersky, and R. Zemel. Prototypical networks for few-shot learning. In *Annual Conference on Neural Information Processing Systems*, pages 4077–4087, 2017.
- [63] D. Stutz, M. Hein, and B. Schiele. Disentangling adversarial robustness and generalization. In *Proceedings of the IEEE/CVF Conference on Computer Vision and Pattern Recognition*, pages 6976–6987, 2019.
- [64] M. Sugiyama and A. J. Storkey. Mixture regression for covariate shift. In *Annual Conference on Neural Information Processing Systems*, pages 1337–1344, 2007.
- [65] C. Szegedy, V. Vanhoucke, S. Ioffe, J. Shlens, and Z. Wojna. Rethinking the inception architecture for computer vision. In *Proceedings of the IEEE/CVF Conference on Computer Vision and Pattern Recognition*, pages 2818–2826, 2016.
- [66] C. Szegedy, W. Zaremba, I. Sutskever, J. Bruna, D. Erhan, I. Goodfellow, and R. Fergus. Intriguing properties of neural networks. In *International Conference on Learning Representations*, 2014.
- [67] S. Thrun and L. Pratt. *Learning to learn*. Springer Science & Business Media, 2012.
- [68] I. Tolstikhin, O. Bousquet, S. Gelly, and B. Schölkopf. Wasserstein auto-encoders. In *International Conference on Learning Representations*, 2018.
- [69] C. Villani. *Topics in optimal transportation*. Number 58. American Mathematical Soc., 2003.
- [70] O. Vinyals, C. Blundell, T. Lillicrap, and D. Wierstra. Matching networks for one shot learning. In *Annual Conference on Neural Information Processing Systems*, pages 3630–3638, 2016.
- [71] R. Volpi, H. Namkoong, O. Sener, J. C. Duchi, V. Murino, and S. Savarese. Generalizing to unseen domains via adversarial data augmentation. In *Annual Conference on Neural Information Processing Systems*, pages 5334–5344, 2018.
- [72] H. Wang, S. Ge, Z. Lipton, and E. P. Xing. Learning robust global representations by penalizing local predictive power. In *Annual Conference on Neural Information Processing Systems*, pages 10506–10518, 2019.
- [73] P. Warden. Speech commands: A dataset for limited-vocabulary speech recognition. *arXiv preprint arXiv:1804.03209*, 2018.
- [74] X. Xu, X. Zhou, R. Venkatesan, G. Swaminathan, and O. Majumder. d-sne: Domain adaptation using stochastic neighborhood embedding. In *Proceedings of the IEEE/CVF Conference on Computer Vision and Pattern Recognition*, pages 2497–2506, 2019.
- [75] J. Yoon, T. Kim, O. Dia, S. Kim, Y. Bengio, and S. Ahn. Bayesian model-agnostic meta-learning. In *Annual Conference on Neural Information Processing Systems*, pages 7332–7342, 2018.
- [76] S. Zagoruyko and N. Komodakis. Wide residual networks. In *Proceedings of the British Machine Vision Conference*, 2016.
- [77] H. Zhang, M. Cisse, Y. N. Dauphin, and D. Lopez-Paz. mixup: Beyond empirical risk minimization. In *International Conference on Learning Representations*, 2018.
- [78] L. Zhao, T. Liu, X. Peng, and D. Metaxas. Maximum-entropy adversarial data augmentation for improved generalization and robustness. In *Annual Conference on Neural Information Processing Systems*, pages 14435–14447, 2020.
- [79] L. Zhao, X. Peng, Y. Chen, M. Kapadia, and D. N. Metaxas. Knowledge as priors: Cross-modal knowledge generalization for datasets without superior knowledge. In *Proceedings of the IEEE/CVF Conference on Computer Vision and Pattern Recognition*, pages 6528–6537, 2020.